

The Molecular Structure of SEBS Grafted with Maleic Anhydride through Ultrasound Initiation*

Xian-long Zhang, Hong Wu** and Shao-yun Guo**

The State Key Laboratory of Polymer Materials Engineering, Polymer Research Institute of Sichuan University, Chengdu 610065, China

Abstract The molecular structure of SEBS grafted with maleic anhydride (SEBS-g-MAH) through ultrasound initiation was investigated by nuclear magnetic resonance (NMR). It can be confirmed that the grafting groups mainly exist on the terminus of the ultrasound initiated SEBS-g-MAH. However, it was difficult to detailedly confirm the block of the SEBS on which MAH is grafted through characterization of $^1\text{H-NMR}$ due to the complex structure of the SEBS. Moreover, the temperature-dependent infrared spectra of the ultrasound initiated SEBS-g-MAH were also analyzed by the perturbation correlation moving window 2D (PCMW2D) correlation spectroscopy. It could confirm that the broken point existed at the joint between poly(ethylene-co-1-butene) (EB block) and polystyrene block (S block). Therefore, the grafting groups were attached to not only the S block but also the EB block. In addition, in order to well understand the aggregation structure of the ultrasound initiated SEBS-g-MAH, the possible grafting mechanism and aggregation model of the ultrasound initiated SEBS-g-MAH at room temperature were also proposed.

Keywords: Ultrasound; Molecular structure; SEBS-g-MAH; Grafting.

INTRODUCTION

Styrene-*b*-(ethylene-co-1-butene)-*b*-styrene (SEBS) tri-block copolymer as a thermoplastic elastomer has received much attention because of its good mechanical properties, thermal stability and reuse possibility. SEBS can be used not only as an elastomer independently, but also as a compatibilizer to enhance the mechanical properties of polystyrene/polyolefin^[1–3]. Moreover, SEBS grafted with functional monomer such as maleic anhydride (MAH) (SEBS-g-MAH), has been also used as compatibilizer in order to reduce the interfacial tension of immiscible polymer blends^[4, 5].

Generally, the peroxide such as dicumyl peroxide (DCP) was utilized to initiate the grafting reaction between polymer and MAH^[6, 7]. E. passaglia and co-workers found that cross-linking polymers were easily formed by peroxide initiation in melt state during functionalization of SEBS^[8]. Besides the functionalization reaction itself, the suppression or avoidance of the side reactions was also of practical interest since the side reactions could worsen the rheological properties and processing characteristics as well as the mechanical properties of the functionalized polymer^[9–12].

In recent years, ultrasound has been introduced as a novel technology to polymer processing. High-power ultrasound waves can cause the scission of the polymer chains to form macro-radicals, which will induce the

* This work was financially supported by the National Natural Science Foundation of China (Nos. 51273132, 50933004 and 51121001).

** Corresponding authors: Hong Wu (吴宏), E-mail: wh@scu.edu.cn

Shao-yun Guo (郭少云), E-mail: nic7702@scu.edu.cn

Received October 29, 2014; Revised December 8, 2014; Accepted December 10, 2014

doi: 10.1007/s10118-015-1645-8

functionalization reaction with less cross-linking side reactions^[13–16]. Our previous studies showed that the gel content of the products initiated by ultrasound was lower than that by the peroxide, and the molecular structure of the ultrasound initiated products was characterized by ¹H-NMR spectroscopy, indicating that the maleic anhydride ring was attached to the chain terminus of the ultrasound initiated products^[17].

In our previous study, ultrasound can be also utilized to initiate functionalization reaction of SEBS with MAH, and the experimental results indicated that ultrasound could cause chain scission of SEBS and suppress the cross-linking side reaction to gain functionalized products, which had less gel content and high grafting ratio^[18]. In order to make ultrasound initiated SEBS-g-MAH to have a promise future in polymer blends as a good compatibilizer, it was necessary to understand well the molecular structure of ultrasound initiated SEBS-g-MAH.

Generally, besides, nuclear magnetic resonance (NMR) and gel permeation chromatography (GPC), infrared spectroscopy (IR) as a useful tool was utilized to characterize the molecular structure of polymers. However, the information of general IR was limited. To obtain much more information, the IR spectra were analyzed by two dimensional correlation spectroscopy. In 2006, Morita proposed perturbation correlation moving window two-dimensional (PCMW2D) correlation spectroscopy^[19–21]. Temperature-dependent IR spectra of several kinds of environmental friendly polymers such as cellulose and polyhydroxyalkanoates (PHAs) were analyzed successfully through PCMW2D correlation spectroscopy^[22, 23].

In addition, due to the different solubility parameter between the polystyrene (S block) and the poly(ethylene-co-1-butene) (EB block) of SEBS, phase separation is a certain physical characteristic, and Fig. 1(A) shows the aggregation state of SEBS^[24]. According to our previous work^[18], the macro-radicals, which are obtained through the chain scission of the SEBS under high-power ultrasound, react with MAH so that functionalization reaction is carried out. Therefore, the grafting groups are mainly attached to the end of molecular chains. In our opinions, there are several possible aggregation states of the ultrasound initiated SEBS-g-MAH. State B (Fig. 1B) suggests that MAH is only attached to the EB block; State C (Fig. 1C) suggests that MAH is only attached to the S block; State D (Fig. 1D) suggests that MAH is attached not only to the EB block but also to the S block. If the thermo-responsive behavior of the grafting group is coincided with that of any block of the copolymer, the grafting group is grafted on that block. Therefore, to confirm the block of the SEBS on which the grafting groups are grafted, it is of interest to obtain thermo-responsive behavior of the grafting group. In addition, the PCMW2D correlation analysis of temperature-dependent infrared spectra of the ultrasound initiated SEBS-g-MAH could reveal different thermo-responsive behaviors of the tri-block copolymer under heat perturbation.

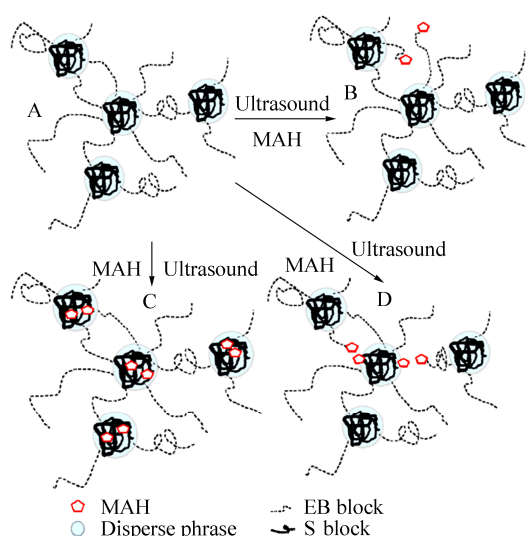


Fig. 1 Possible aggregation states of SEBS and ultrasound initiated SEBS-g-MAH

In this paper, the temperature dependent infrared spectra of the ultrasound initiated SEBS-g-MAH is analyzed by perturbation correlation moving-window 2D correlation spectroscopy. Moreover, the molecular structure of the SEBS-g-MAH was also analyzed by $^1\text{H-NMR}$. In addition, in an attempt to correctly understand the main aggregation state of the ultrasound initiated SEBS-g-MAH, a model of the aggregation state of the ultrasound initiated SEBS-g-MAH is proposed. Finally, the possible grafting mechanism is also proposed.

EXPERIMENTAL

Materials and Equipment

SEBS used in this study is 6150, which comes from TSRC Co., Ltd. (China), and the EB block and S block ratio is 71/29. All other chemicals including maleic anhydride (MAH) are of reagent grade and are used without further purification. The hydrocarbon oil ($\text{C}_{16}\text{H}_{34}\sim\text{C}_{21}\text{H}_{44}$ *N*-alkanes mixture, molecular weight 226–296, kinematic viscosity of types: 15–24 mm^2/s at 40 °C) used as plasticizer is of industrial grade and supplied by Chengdu Xinlong Chemical Co., Ltd. (China). A special ultrasound extruding reactor developed in our lab, whose schematic diagram is shown in Fig. 2, is used to prepare SEBS-g-MAH, and much more detail information about the ultrasound extruding reactor has been described in Refs. [17] and [18]. The die is a special horn capillary (length/diameter (L/D) = 10) attached to a single screw extruder with 25 mm diameter and a length to diameter ratio L/D = 30. The maximum power output and fixed frequency of the generator are 300 W and 20 kHz. The ultrasound power is 200 W, and the temperature profile from feed zone to die zone is set to 80, 180, 180 and 180 °C, respectively. The screw rotation speed is fixed at 10 r/min.

The functionalized products are purified by the following steps. Each functionalized product (~2 g) is heated in 200 mL refluxing xylene for 1 h then filtered into 400 mL acetone. The acetone-insoluble polymer is refluxed with acetone for 4 h, and then dried under vacuum at 60 °C for 12 h. The grafting percentage of SEBS-g-MAH, which is measured by acid-base titration, is 0.91%, and the detailed preparation of the ultrasound initiated SEBS-g-MAH is described in Ref. [18].

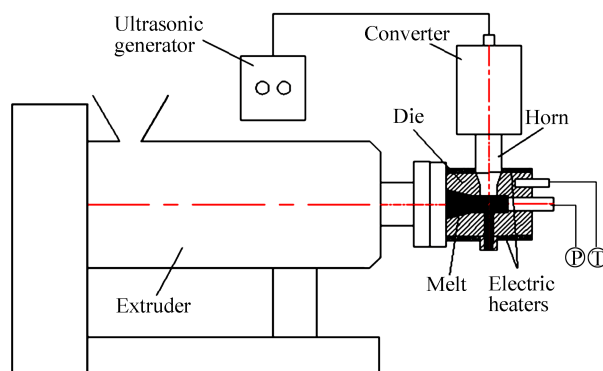


Fig. 2 Schematic diagram of the ultrasonic extruding reactor

Nuclear Magnetic Resonance (NMR)

$^1\text{H-NMR}$ spectra (400 MHz) of the SEBS-g-MAH and SEBS are recorded with a Bruker Avance NMR apparatus at room temperature. The SEBS-g-MAH sample is prepared by dissolving the SEBS-g-MAH (about 15 mg) into CDCl_3 (0.5 mL) in a NMR tube. Similarly, the pure SEBS sample is prepared through the same method. The spectra are referenced relative to TMS using the solvent signal as an internal standard.

FTIR Spectroscopy

The SEBS-g-MAH is spread on one side of a KBr disk *via* solvent casting from 20 g/L xylene solution. The thickness of the sample, which is measured by a Coatstest-1000 nonferrous digital coating thickness gauge (Jinan SanQuan Experiment Instrument Co., Shandong, China), is ~10 μm . The KBr disk (0.8 mm thick), together with samples, are dried in a vacuum oven at 70 °C for 60 min. the samples was conducted ordinary FTIR

spectroscopy (transmission model) measurements with a Nicolet-IS10 (Thermo Electron Co., USA) spectrometer.

The SEBS-g-MAH film disk sample is placed into a temperature control instrument, which including programmed heating cell and circulating water jacket cooling system. The temperature-dependent absorbance IR spectra are collected by a Nicolet-IS10 (Thermo Electron Co., USA) spectrometer. The spectral resolution is 4 cm^{-1} and scan number of each spectrum is 10, and the time interval between two successive spectra was about 10 s. The SEBS-g-MAH film sample is protected by dried high-purity nitrogen gas during the measurement. The measurement temperature range is from $25\text{ }^{\circ}\text{C}$ to $150\text{ }^{\circ}\text{C}$, and the heating rate is 5 K/min .

PCMW2D Correlation Analysis

The theory of the PCMW2D correlation spectroscopy has been described in Ref. [17], and all the PCMW2D correlation spectra are calculated by two-dimensional correlation spectra program, which is developed by our group based on MATLAB 7.0. The contour images of the PCMW2D correlation spectroscopy are draw through Origin Pro 8.0. During the calculation, the window size is 11. The 5% autocorrelation intensity of PCMW2D correlation spectroscopy is regarded as noise and is cut off. The filled gray and unfilled areas represent the positive and negative correlation intensity, respectively.

RESULTS AND DISCUSSION

Nuclear Magnetic Resonance (NMR)

The $^1\text{H-NMR}$ spectra of the pure SEBS and the ultrasound initiated SEBS-g-MAH are shown in Fig. 3. The signals for the CH_3- ($\delta=0.82$), $-(\text{CH}_2)_n-$ ($\delta=1.24$) and benzene ring ($\delta=6.46$, $\delta=6.43$, $\delta=6.57$, $\delta=7.08$, $\delta=7.26$) indicate the fundamental peaks of the SEBS^[25]. Some weak signals appear at $\delta=2-5.5$, indicating the different structure between pure SEBS and ultrasound initiated SEBS-g-MAH. The small peak of **a**, **b** and **c** at $\delta=3.51$, 2.73 and 3.05 could be assigned to the methylene proton and the two methylene protons of the succinic anhydride ring blocked on the end chain (the structure formula **I**)^[26-28], respectively. Meanwhile, the small peak **a** ($\delta=3.51$) could also be assigned to the two methylene protons of the succinic anhydride ring blocked in the chain (the structure formula **II**). In addition, the signal **d** at $\delta=4.04$ is not very obvious. Moreover, the signals **e** ($\delta=5.09$), **d** ($\delta=4.04$) and **f** ($\delta=5.31$) are attributed to the structure of formula **III**^[26-28]. Therefore, it can be confirmed that the grafting groups mainly exist on the terminus of the ultrasound initiated SEBS-g-MAH. However, it is difficult to detailedly confirm the block of SEBS on which MAH is grafted through characterization of $^1\text{H-NMR}$ due to the complex structure of SEBS.

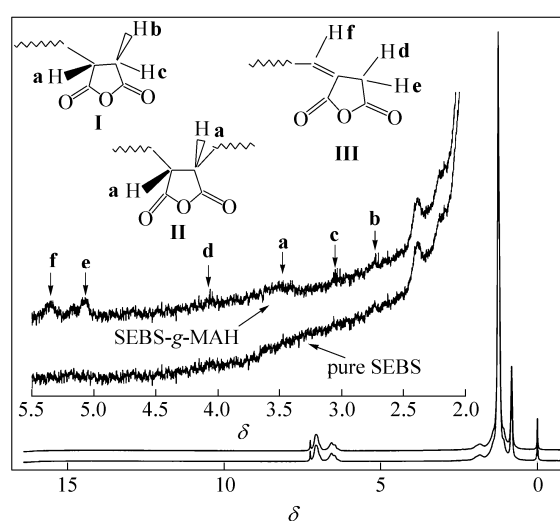


Fig. 3 The $^1\text{H-NMR}$ spectra of pure SEBS and ultrasound initiated SEBS-g-MAH

PCMW2D Correlation Analysis

The melting of weak crystalline of EB block

In order to reveal much more information about structure of the ultrasound initiated SEBS-g-MAH, the temperature dependent infrared spectra of the ultrasound initiated SEBS-g-MAH are analyzed by perturbation correlation moving window 2D correlation spectroscopy. Figure 4 shows Π_Φ synchronous (a) and Π_Ψ asynchronous (b) PCMW2D correlation IR spectra of the ultrasound initiated SEBS-g-MAH in the 710–730 cm^{-1} region. The band around 721 cm^{-1} is assigned to C–H rocking vibration of the $-\text{CH}_2-$ in EB blocks, and corresponds to the feature peak of weak crystalline EB blocks of SEBS-g-MAH^[29, 30]. According to Figs. 4(a) and 4(b), $\Pi_\Phi(721 \text{ cm}^{-1}, 32 \text{ }^\circ\text{C}) < 0$ and $\Pi_\Psi(721 \text{ cm}^{-1}, 32 \text{ }^\circ\text{C}) > 0$ indicate that the spectral intensity decreases with increasing temperature according to the rules of PCMW2D correlation spectroscopy proposed by Morita^[19]. Figure 4(c) shows that the intensity of the band around 721 cm^{-1} truly decreases with increasing temperature (not all spectra are shown here to facilitate clear visualization). Because of the different samples and experimental conditions, melting temperature range of the weak crystalline EB of SEBS is from 25 $^\circ\text{C}$ to 55 $^\circ\text{C}$ ^[31, 32]. Apparently, 32 $^\circ\text{C}$ obtained from the PMW2D correlation analysis of the ultrasound initiated SEBS-g-MAH is in the region 25–55 $^\circ\text{C}$. Therefore, 32 $^\circ\text{C}$ as a melting temperature of the extraordinary weak crystalline EB blocks of the ultrasound initiated SEBS-g-MAH is reasonable.

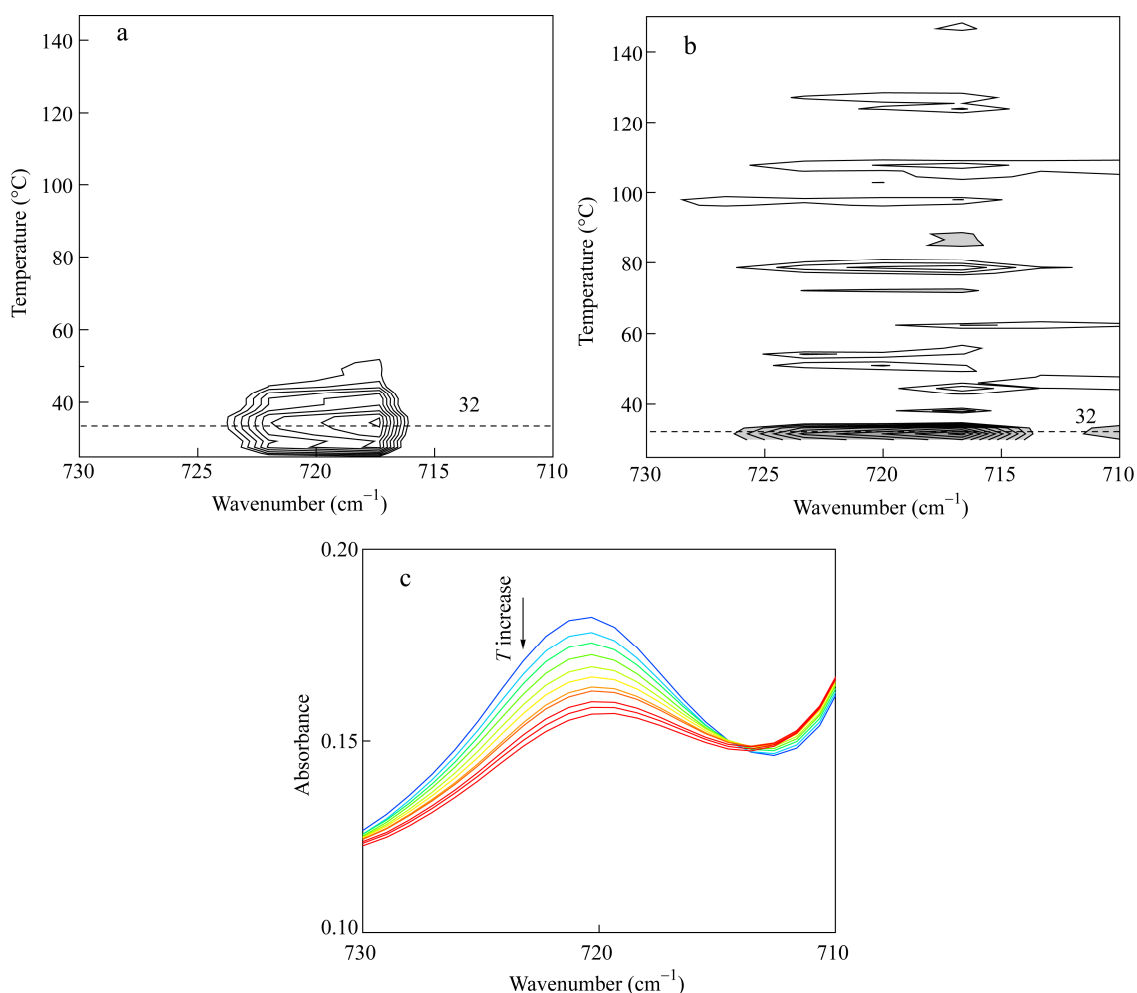


Fig. 4 Π_Φ synchronous (a) and Π_Ψ asynchronous (b) PCMW2D correlation IR spectroscopy of ultrasound initiation SEBS-g-MAH base on the temperature-dependent IR spectra (c) (25–150 $^\circ\text{C}$) in the region 710–730 cm^{-1} (The heating rate is 5 K/min.)

The thermo-responsive behaviors of the S and EB block

Figure 5 shows that Π_ϕ synchronous (a) and Π_ψ asynchronous (b) PCMW2D correlation IR spectra of the ultrasound initiated SEBS-g-MAH in the region 2800–3000 cm^{-1} , and Fig. 5(c) shows the temperature-dependent IR spectra. The band around 2852 cm^{-1} is assigned to the C–H symmetry stretching vibration of $-\text{CH}_2-$ of EB block. Several synchronous correlation peaks are obviously observed at 29, 99 and 115 $^\circ\text{C}$ in Fig. 5(a). The Π_ϕ (2852 cm^{-1} , 29 $^\circ\text{C}$) negative correlation peak is found at 29 $^\circ\text{C}$, which is close to the melting temperature of the extraordinary weak crystalline EB blocks. Therefore, the Π_ϕ (2852 cm^{-1} , 29 $^\circ\text{C}$) negative correlation peak may result from melt of extraordinary weak crystalline EB (31 $^\circ\text{C}$) according to the analysis of the Figs. 4(a), 4(b) and 4(c). Moreover, the band around 2923 cm^{-1} is assigned to the C–H symmetry stretching vibration of $-\text{CH}_2-$ of the S block^[33]. The negative peaks (Π_ϕ (2852 cm^{-1} , 115 $^\circ\text{C}$), Π_ϕ (2923 cm^{-1} , 115 $^\circ\text{C}$)) are observed at 115 $^\circ\text{C}$, and these two peaks maybe result from glass transition of S block. This temperature (115 $^\circ\text{C}$) is close to temperature that other researcher obtained^[24]. Therefore, it is reasonable to confirm this temperature (115 $^\circ\text{C}$) as glass transition temperature of the S blocks of the ultrasound initiated SEBS-g-MAH. The negative peak Π_ϕ (2852 cm^{-1} , 115 $^\circ\text{C}$) is attributed to the movements of EB block, which connected with S block and caused by glass transition of S blocks. Moreover, the negative peak at 99 $^\circ\text{C}$ (Π_ϕ (2852 cm^{-1} , 99 $^\circ\text{C}$)) is observed and would be discussed later in combination with Fig. 6.

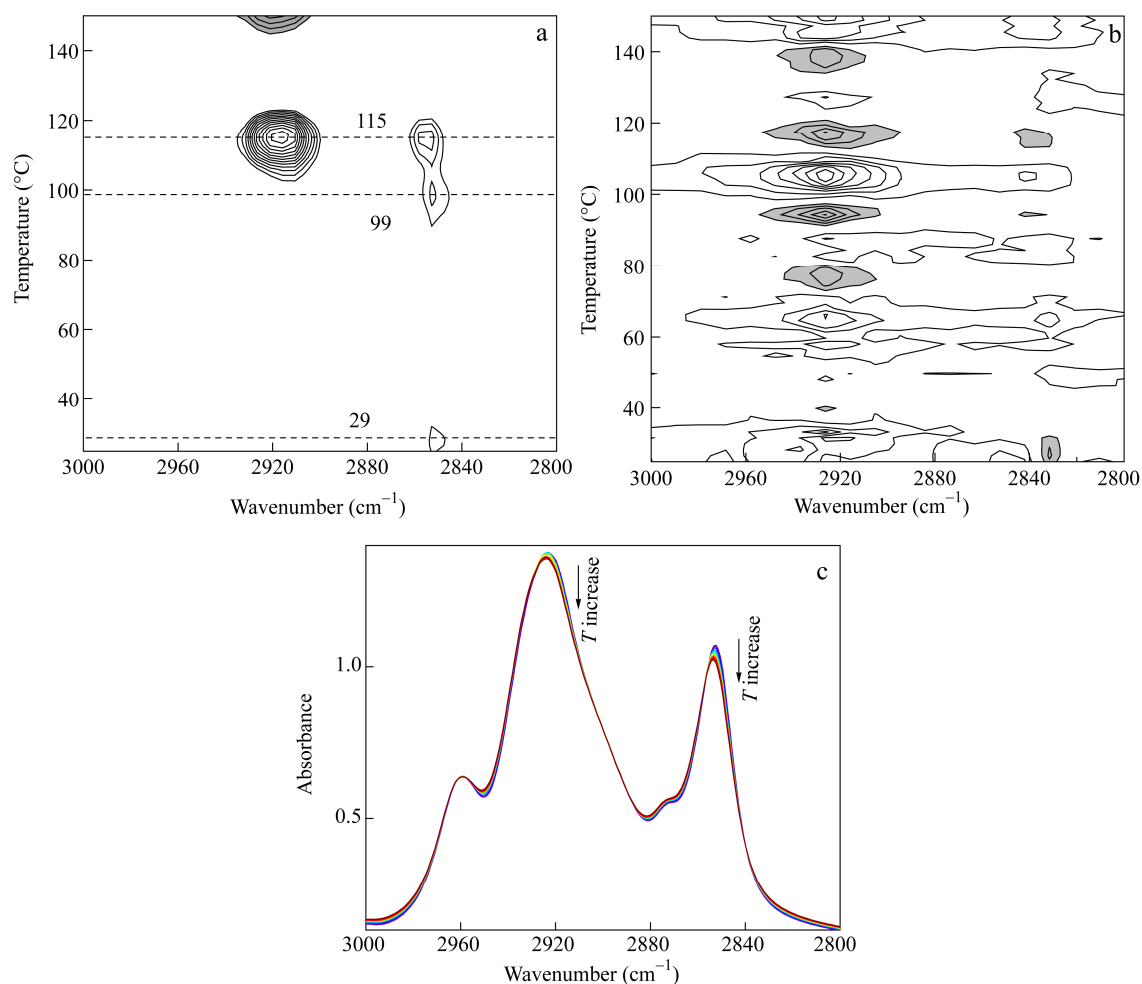


Fig. 5 Π_ϕ synchronous (a) and Π_ψ asynchronous (b) PCMW2D correlation IR spectroscopy of ultrasound initiated SEBS-g-MAH base on the temperature-dependent IR spectra (c) (25–150 $^\circ\text{C}$) in the region 2800–3000 cm^{-1}

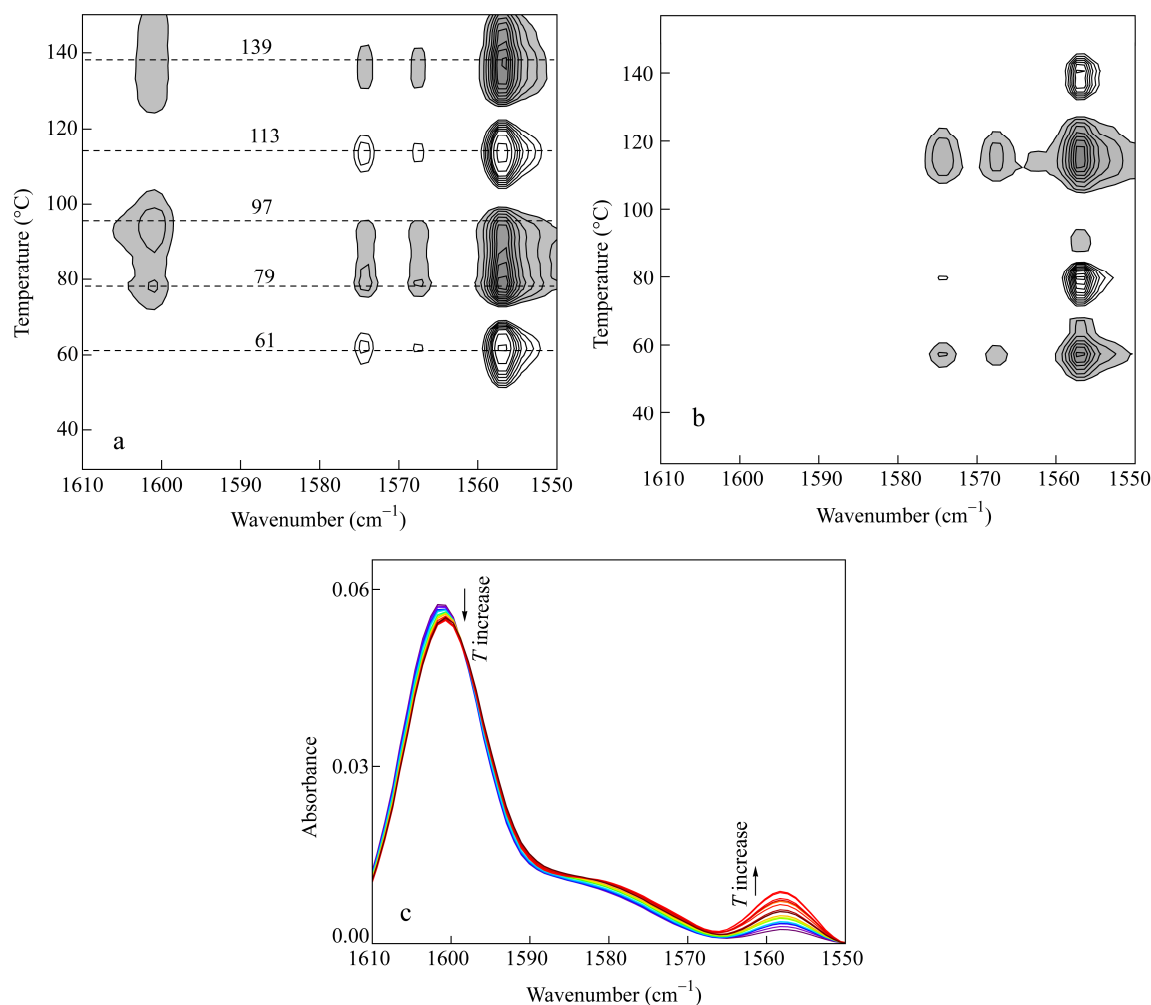


Fig. 6 Π_{ϕ} synchronous (a) and Π_{ψ} asynchronous (b) PCMW2D correlation IR spectroscopy of ultrasound initiated SEBS-g-MAH based on the temperature-dependent IR spectra (c) (25–150 °C) in the region 1550–1610 cm^{-1}

The thermo-responsive behaviors of side benzene rings (S block)

The bands around 1557, 1568, 1575 cm^{-1} are assigned to the overtone or combination vibration of side benzene ring, and the band around 1600 cm^{-1} is assigned to the framework vibration of side benzene ring^[33]. Figure 6(a) shows the Π_{ϕ} synchronous and (b) asynchronous PCMW2D correlation IR spectra of the ultrasound initiated SEBS-g-MAH in the region 1500–1610 cm^{-1} , and temperature-dependent IR spectra are shown in Fig. 6(c). According to results of analysis in Figs. 5(a), 5(b) and 5(c), the temperature 113 °C is close to the glass transition of the S blocks (115 °C). Therefore, the 113 °C Π_{ϕ} (1557 cm^{-1} , 113 °C), Π_{ϕ} (1568 cm^{-1} , 113 °C) and Π_{ϕ} (1575 cm^{-1} , 113 °C) may result from the glass transition of the S blocks. Moreover, the movements of side benzene ring are ascribed to the heat enthalpy relaxation of S block when the temperature is below temperature of glass transition of S block (115 °C). Therefore, there are only movements of side benzene ring at 61, 79 and 97 °C. In addition, the side benzene ring moves only in the local area at 141 °C because the movement of fundamental chain of the ultrasound initiated SEBS-g-MAH is not observed in Fig. 5.

The thermo-responsive behaviors of the grafting groups

Figure 7 shows that (a) Π_{ϕ} synchronous and (b) Π_{ψ} asynchronous PCMW2D correlation IR spectra of the ultrasound initiated SEBS-g-MAH based on the temperature-dependent IR spectra (c) in the region 1700–1800 cm^{-1} . The bands around 1786 and 1721 cm^{-1} are assigned to the MAH and –COOH (MAH

hydrolyzed group absorption band) characteristic absorption bands, respectively^[34, 35]. In Fig. 7(a) the negative peaks observed at 32 °C may be induced by melting of weak crystalline EB blocks in SEBS-g-MAH according to the analysis in Fig. 4, indicating that the thermo-responsive behavior of grafting groups is coincided with melting of the weak crystalline EB blocks of the ultrasound initiated SEBS-g-MAH, and that is to say, grafting groups exist on EB blocks. Moreover, the negative and positive peaks are observed at 61 and 79 °C in Fig. 7(a). Meanwhile, side benzene ring relaxation of SEBS-g-MAH is also observed at 61 and 79 °C in Fig. 6(a), indicating that the movement of grafting groups is coincided with that of the benzene ring of the ultrasound initiated SEBS-g-MAH. The correlation peaks (Π_ϕ (1786 cm^{-1} , 113 °C), Π_ϕ (1721 cm^{-1} , 113 °C)) at 113 °C may be the consequence of glass transition of the S blocks. However, the positive and negative of correlation peaks in Figs. 4, 5 and 6 are not coincided with each other because different bands have different changes of the spectral intensity under heat perturbation. Moreover, the negative correlation peaks at 139 °C is attributed to the benzene ring movement in local areas according to analysis at Fig. 6.

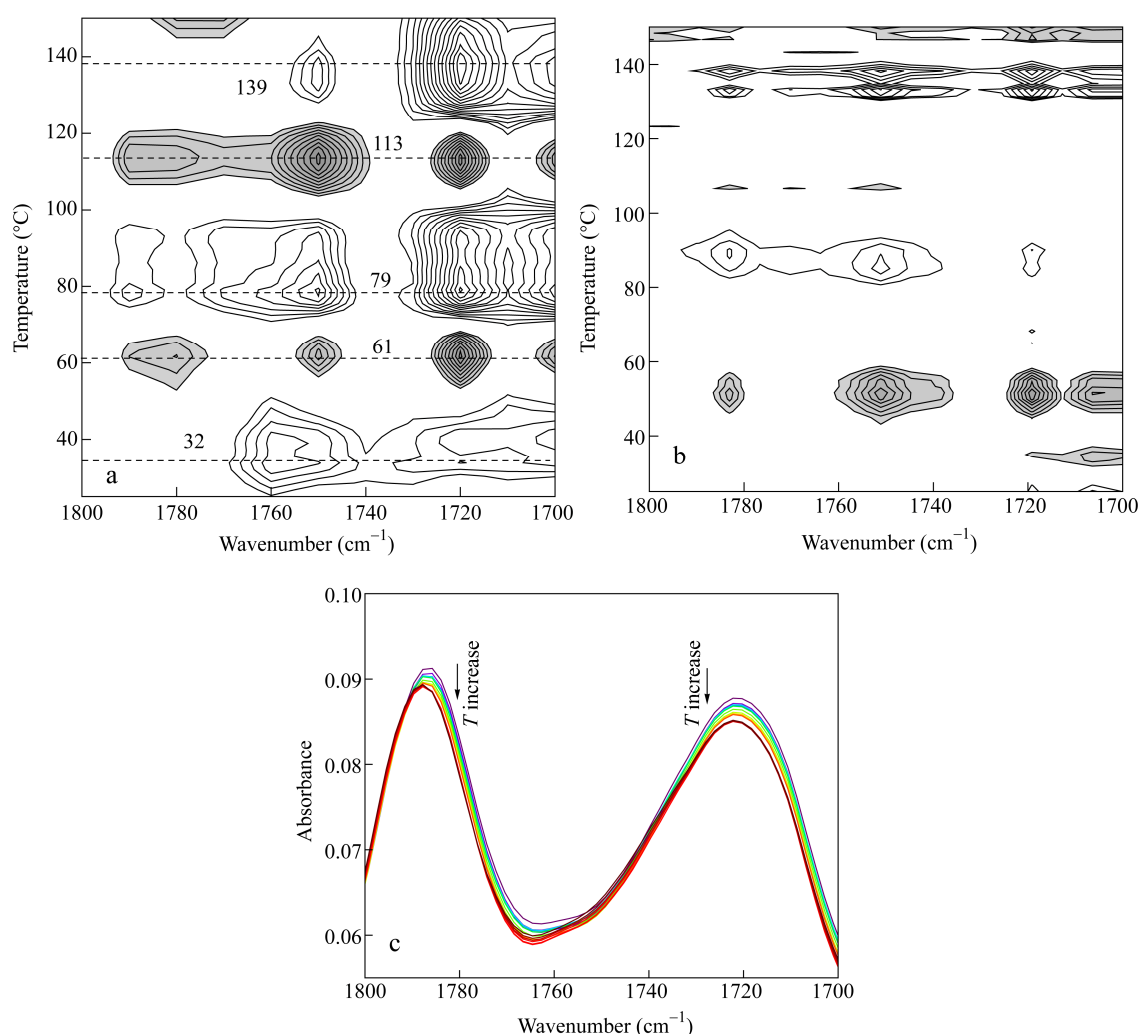


Fig. 7 Π_ϕ synchronous (a) and Π_ψ asynchronous (b) PCMW2D correlation IR spectroscopy of ultrasound initiated SEBS-g-MAH based on the temperature-dependent IR spectra (c) (25–150 °C) in the region 1700–1800 cm^{-1}

According to analysis of Figs. 4, 5, 6 and 7, Table 1 shows temperature responses of the grafting group (MAH), EB block and S block, indicating that the thermo-responsive behavior of the grafting groups are coincided not only with that of the EB blocks but also with that of the S blocks. Therefore, the grafting groups should exist not only on the EB blocks but also on S blocks.

Table 1. Temperature responses of the grafting group (MAH), EB block and S block

MAH (°C)	EB block (°C)	S block (°C)
32	31	61
61	–	79
79	–	97
113	–	115

Aggregation Model

According to PCMW2D correlation IR spectroscopy analysis the grafting groups exist not only on EB blocks but also on S blocks, in an attempt to understand the main aggregation state of the ultrasound initiated SEBS-g-MAH correctly, a possible model of the aggregation state of the ultrasound initiated SEBS-g-MAH is proposed.

Figure 8(a) shows the aggregation model of SEBS at room temperature, and this aggregation model has been report in literature^[24]. According to this report, there is a unique location, which is the interface between the S and EB blocks, and this interface is a transitional region. Therefore, the chain segment of S and EB block coexist. However, it is of interest to know the aggregation model after functionalized SEBS with MAH. According to the PCMW2D analysis of the temperature dependent infrared spectra of ultrasound initiated SEBS-g-MAH, the movements of grafting groups are coincided with not only those of S blocks, but also EB blocks. Therefore, the grafting groups mainly concentrate on the interface between S block and EB block. In presence of ultrasound waves, the molecular chains of SEBS are broken down, and the broken point existed at the joint between S and EB blocks. The main reasons may be that on the one hand, EB blocks have higher molecular weight and better flexibility than S blocks. On the other hand, S blocks have more rigid and longer chain segment than the EB blocks. Therefore, the EB blocks keep pace with the changes of ultrasound vibration more easily than S blocks, and then weak points are the joints between EB blocks and S blocks, where molecular chains of SEBS break down in the presence of high-power ultrasound waves. Meanwhile, the macromolecular radicals are formed, following that the macromolecular radicals react with MAH. Therefore, the grafting groups should exist not only on the EB block but also on the S block. Based on the above analysis of the temperature dependent infrared spectra of the ultrasound initiated SEBS-g-MAH, the aggregation model of ultrasound initiated SEBS-g-MAH at room temperature is proposed in Fig. 8(b).

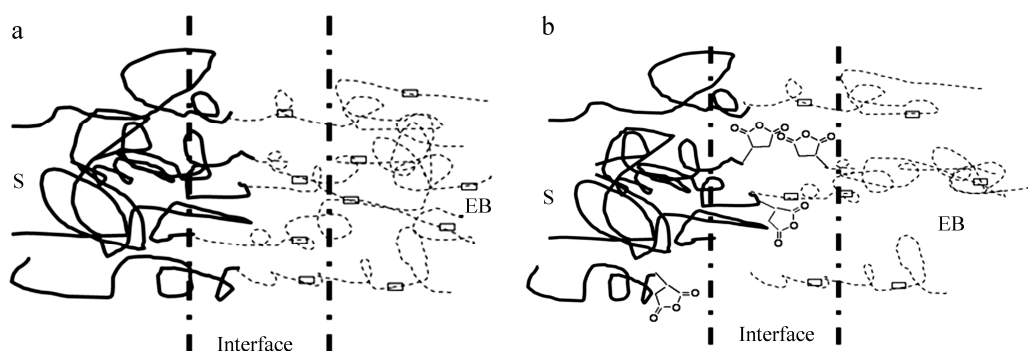
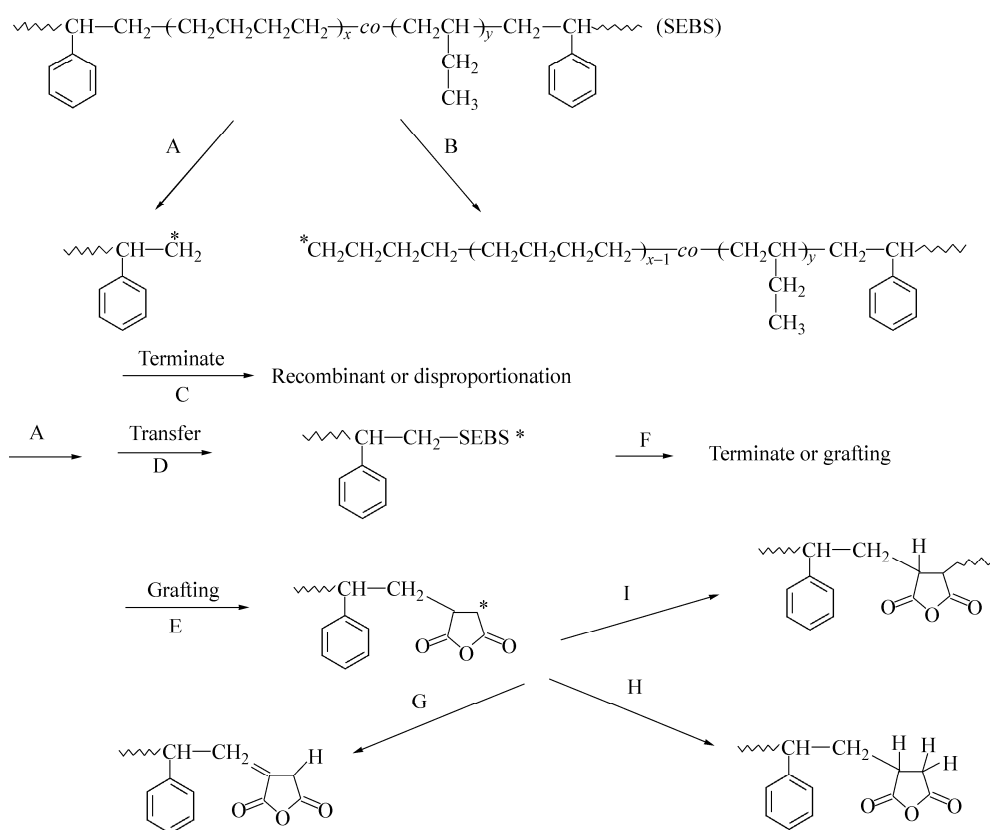


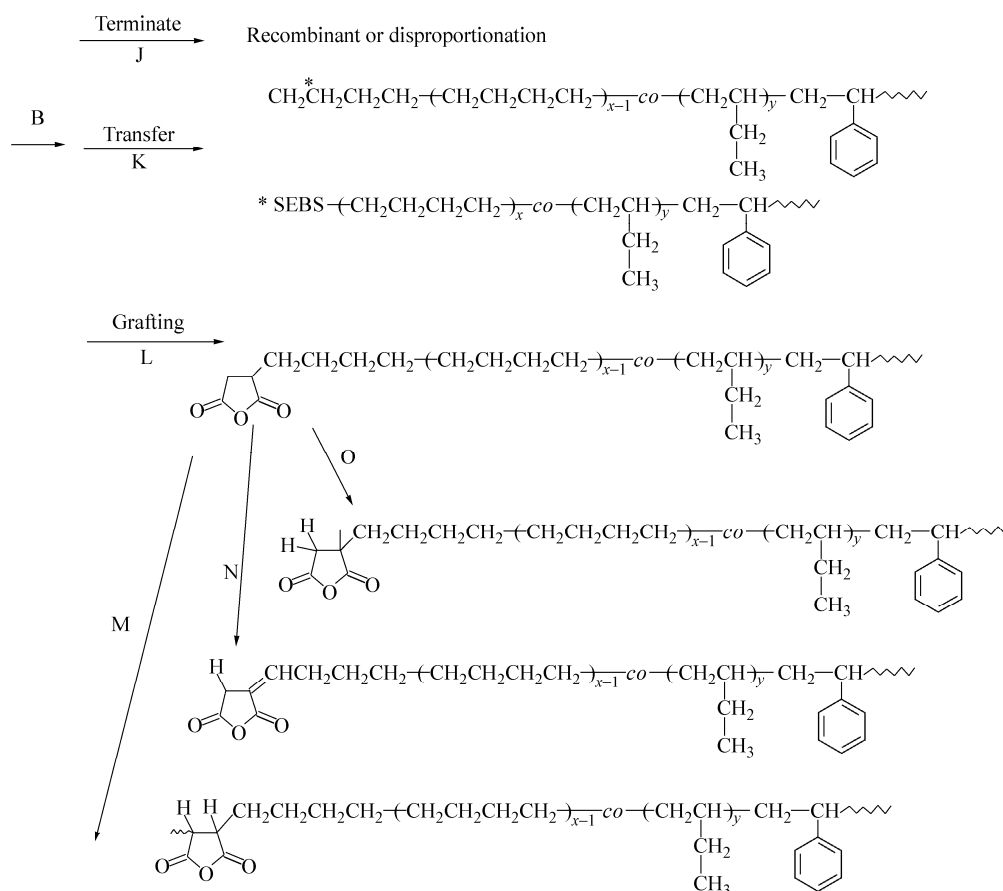
Fig. 8 Sketch map of SEBS (a) and ultrasound initiated SEBS-g-MAH (b) at room temperature. The thick dash lines represent interface areas, the solid lines represent polystyrene (S block), and the fine dash lines represent poly(ethylene-co-1-butene) (EB block), respectively. The small rectangle boxes drilled by EB molecular chains stand for very weak crystalline EB block regions.

Because of the limitation of the temperature control system in the IR sample cell, the temperature range of the IR experiment is only from 25 °C to 150 °C in this paper. In fact, the glass transition temperature of the EB blocks is from -50 °C to -60 °C. If the experimental temperature range is from -100 °C to 0 °C, more information will be obtained by PCMW2D analysis of the temperature dependent infrared spectra of ultrasound initiated SEBS-g-MAH under heat stimulation. This is employed in our further study.

The Possible Grafting Mechanism

Based on analysis results of the ¹H-NMR and PCMW2D correlation IR spectra, a simple grafting reaction mechanism initiated by ultrasound initiation was proposed. Scheme 1 shows the main reaction routes for MAH grafting onto SEBS in melt state through ultrasonic initiation. The chain scission of the SEBS under ultrasonic wave action was the dominating step (reaction route A, B). The reaction mainly consisted of transfer (A+K+D), recombination (F) and reaction of the macromolecular radicals with MAH (E+I+J+H, L+M+N+O) and terminated reaction (C+J). Finally, the products with functional groups grafting on the end of chains were obtained under ultrasonic wave action.





Scheme 1 The reaction mechanism of the SEBS-g-MAH prepared by ultrasound initiation

CONCLUSIONS

The molecular structure of the ultrasound initiated SEBS-g-MAH is investigated by $^1\text{H-NMR}$. It can be confirmed that the grafting groups mainly exist on the terminus of the ultrasound initiated SEBS-g-MAH. However, it is difficult to detailedly confirm the block of SEBS on which MAH is grafted through characterization of $^1\text{H-NMR}$ due to the complex structure of the SEBS. Moreover, through analysis of PCMW2D correlation spectra of the ultrasound initiated SEBS-g-MAH, the thermo-responsive behavior of the grafting groups is coincided not only with that of the EB blocks but also that of the S blocks. Therefore, the grafting groups should exist not only on the EB block but also on the S block. Based on analysis results of the $^1\text{H-NMR}$ and PCMW2D correlation IR spectra, a simple grafting reaction mechanism initiated by ultrasound initiation and possible aggregation model of ultrasound initiated SEBS-g-MAH at room temperature are proposed.

REFERENCES

- 1 Fayt, R., Jerome, R. and Teyssie, P., *J. Polym. Sci., Part B: Polym. Phys.*, 1989, 27(3): 775
- 2 Zheng, J.Z., Zhou, X.P., Ying, J.R., Xie, X.L. and Mai, Y.W., *Chinese J. Polym. Sci.*, 2009, 27(5): 685
- 3 Li, T., Topolkarav, A., Hiltner, A., Baer, E., Ji, X.Z. and Quirk, R.P., *J. Polym. Sci., Part B: Polym. Phys.*, 1995, 33(4): 667
- 4 Matos, M., Favis, B.D. and Lomellini, P., *Polymer*, 1995, 36(20): 3899

- 5 Majumdar, B., Keskkula, H. and Paul, D.R., *Polymer*, 1994, 35(25): 1387
- 6 Zhao, G.D., Xu, J.M., Xie, S.P., Liu, X.F., Yang, J.S. and Xu, L.H., *Chinese J. Polym. Sci.*, 2013, 31(9): 1271
- 7 Nipithakul, T., Watthanachote, L. and Kalapat, N., *Chinese J. Polym. Sci.*, 2012, 30(2): 181
- 8 Passaglia, E., Ghetti, S., Picchioni, F. and Ruggeri, G., *Polymer*, 2000, 41(12): 4389
- 9 Wang, X.L., *Chinese J. Polym. Sci.*, 2012, 30(3): 415
- 10 Wang, J.H., Zhu, L.P., Yi, Z., Li, J.H. and Zhu, B.K., *Chinese J. Polym. Sci.*, 2012, 30(2): 173
- 11 Ho, R.M., Su, A.C., Wu, C.H. and Chen, S.I., *Polymer*, 1993, 34(15): 3264
- 12 Wu, C.H. and Su, A.C., *Polym. Eng. Sci.*, 1991, 31(23): 1629
- 13 Isayev, A.I., Chen, J. and Tukachinsky, A., *Rubber. Chem. Technol.*, 1995, 68(2): 267
- 14 Tukachinsky, A., Schworm, D. and Isayev, A.I., *Rubber. Chem. Technol.*, 1996, 69(1): 92
- 15 Isayev, A.I., Yushanov, S.P. and Chen, J., *J. Appl. Polym. Sci.*, 1996, 59(5): 803
- 16 Isayev, A.I. and Chen, J., US Patent, 5,284,625
- 17 Zhang, Y., Chen, J. and Li, H., *Polymer*, 2006, 47(13): 4750
- 18 Shen, L.Y., Zhang, X.L., Wu, H. and Guo, S.Y., *J. Appl. Polym. Sci.*, 2013, 129(5): 2686
- 19 Morita, S., Shinzawa, H., Noda, I. and Ozaki, Y., *Appl. Spectrosc.*, 2006, 60(4): 398
- 20 Noda, I., *Appl. Spectrosc.*, 1993, 47(9): 1329
- 21 Thomas, M. and Richardson, H., *Vibr. Spectrosc.*, 2000, 24(1): 137
- 22 Watanabe, A., Morita, S. and Ozaki, Y., *Appl. Spectrosc.*, 2006, 60(11): 611
- 23 Watanabe, A., Morita, S. and Ozaki, Y., *Biomacromolecules*, 2006, 7(11): 3164
- 24 Zhou, T., Zhang, A., Zhao, C., Liang, H., Wu, Z. and Xia, J., *Macromolecules*, 2007, 40(25): 9009
- 25 Lipatov, U.S. and Nesterov, A.E., " *Handbook in Physical Chemistry of Polymers* " (in Russian), Naukova Dumka, Kiev, 1984, p. 113
- 26 Zhao, Y. and Sun, Q., *Spectrum analysis and identification of organic chemicals*, University of Science and Technology of China (He fei) Press, 1992, p. 245
- 27 Mrrov, Z. and Velichkova, R., *Eur. Polym. J.*, 1993, 29(4): 597
- 28 Vaccaro, A., Šeřčik, J. and Morbidelli, M., *Polymer*, 2005, 46(4): 1157
- 29 Naka, Y., Nemoto, N. and Song, Y., *J. Polym. Sci., Part B: Polym. Phys.* 2005, 43(12): 1520
- 30 Sworen, J.C., Smith, J.A., Berg, J.M. and Wagener, K.B., *J. Am. Chem. Soc.*, 2004, 126(36): 11238
- 31 Carella, J.M., Graessley, W. and Fetters, L.J., *Macromolecules*, 1984, 17(12): 2775
- 32 Crist, B. and Claudio, E.S., *Macromolecules*, 1999, 32(36): 8945
- 33 Painter, P., Sobkowiak, M. and Park, Y., *Macromolecules*, 2007, 40(5): 1730
- 34 Roover, B.D., Sclavons, M., Carlier, V., Devaux, J., Legras, R. and Momtaz, A., *J. Polym. Sci., Part A: Polym. Chem.*, 1995, 33(5): 829
- 35 Sclavons, M., Laurent, M., Devaux, J. and Carlier, V., *Polymer*, 2005, 46(19): 806